doi.org/10.36721/PJPS.2023.36.3.SP.915-920.1

Control synthesis of mesoporous silica microparticles: Optimization and *in vitro* cytotoxicity studies

Yasir Mehmood[1], Hira Shahid[2], Hammad Yousaf[3*], Umar Farooq[4], Humayun Riaz[3], Rana Khalid Mahmood Arshad[3], Waqas Ahmad[3], Muhammad Affan[3], Muhammad Abu Sufian[3] and Zia Mohy-ud-din Khan[3]

[1]Department of Pharmaceutics, Faculty of Pharmaceutical Sciences, Government College University, Faisalabad, Pakistan
[2]Department of Pharmacology, Faculty of Pharmaceutical Sciences, Government College University, Faisalabad, Pakistan
[3]Rashid Latif College of Pharmacy, Rashid Latif Khan University, Lahore, Pakistan
[4]Faculty of Pharmacy, Grand Asian University, Sialkot, Pakistan

Abstract: The current paper explains how to make mesoporous silica microparticles (MSM) by mixing water and dichloromethane. Several dichloromethane-water ratios were used to adjust the reaction mixture for the first time to easily synthesize mesoporous silica micro particles with regulated particle size. By carefully modifying the concentrations of water and dichloromethane, a higher level of consistency was achieved in the production of micro particles, i.e. to a 2:1 v/v ratio. It was discovered that variations in the dichloromethane-to-water ratios significantly affect the surface roughness and morphologies of mesoporous silica particles along with size. This is most likely because the solvent affects how quickly tetraethyl orthosilicate (TEOS) and how quickly inorganic species polymerize. In all experiments, conditions were maintained the same at 25^{o}C temperature and 1000 rpm. Scanner electron microscopy (SEM), Fourier transform infrared (FTIR) and X-ray powder diffraction (XRD) methods were used to identify the structure of MSM. The *in vitro* cytotoxicity assays showed that the produced particles, which had a diameter of 1.0 m, were safe for usage in the cellular system.

Keywords: Dichloromethane, mesoporous silica micro particles, tetraethyl orthosilicate, cetyltrimethyl ammonium bromide.

INTRODUCTION

Due to their distinct physicochemical characteristics, micro materials have made significant progress over the past two decades, displaying precise and accurate medication delivery and targeting (Singh *et al*., 2014, Sur *et al*., 2019). The main objective of developing smart materials is to create medicines that can increase drug bioavailability at the target areas while lowering the frequency of dose and side effects that are frequently connected to a wide range of medications (Anselmo and Mitragotri, 2019). Inorganic micro particles composed of silicon carbide, silicon nitride, zirconia, alumina and titania have recently been discovered to be effective in biological and pharmacological applications (Krajišnik *et al*., 2017). However, the report on MCM-41 type MSM in 2001 sparked the interest of countless researchers, leading to a significant focus on mesoporous silica micro particles (MSM) for drug delivery. Applications in catalysis, biology and biomedicine have shown significant promise for mesoporous materials, which have enormous specific surface areas and pores with diameters between 5nm to 50nm (Tang *et al*., 2012). MSM are superior to other micro-carriers in a number of ways, including their porous nature, ease of surface functionalization, biocompatibility, low toxicity and ease of production using relatively simple and inexpensive methods (Kumar *et al*., 2018, Li *et al*., 2019). The pharmaceutical industry has made good use of MSM as a versatile carrier that provides tuneable surface characteristics and enough porosity for encapsulating a range of medications (Maggini *et al*., 2016, Manzano and Vallet-Regí, 2020), proteins (Xu *et al*., 2015, Zhou *et al*., 2018), genes (Zhou *et al*., 2018) and enzymes (Zhang *et al*., 2019) for their delivery in different clinical situations. Due to the simplicity of surface functionalization, MSM with a high porosity and large surface area for maintaining a considerable drug's pay-load can target cells particularly where the drug release is required in addition to regulating the drug release at a particular site of interest (He *et al*., 2010, Li *et al*., 2004, Vivero-Escoto *et al*., 2010).

The ability to manage the size, porosity and form of the nanoparticles is one of the key difficulties in the synthesis of MSM. The sol-gel procedure is still the most popular method for producing MSM because it gives exact control over the size, porosity and shape of the nanoparticles. Other methods include chemical vapor deposition, flame spray pyrolysis, micro-emulsion and others (Brinker and Scherer, 2013, Mehmood *et al*., 2019, Mehmood *et al*., 2022a). The soft template approach, which Graham first used to describe the sol-gel process in 1864 (Graham,

*Corresponding author: e-mail: h_y_84@hotmail.com

1864) allows for the low-temperature synthesis of materials that are entirely inorganic or organic-inorganic. (Mehmood *et al*., 2020a, Mehmood *et al*., 2020b, Mehmood *et al*., 2022b). In this study, we proposed a novel method for the one-step synthesis of monodispersed mesoporous silica micro particles (MSM). This technique involved the use of dichloromethane-water mixtures as the reaction media for the first time, sodium hydroxide as the base and cetyltrimethyl ammonium bromide as a structure-directing surfactant. To fully characterize the synthesized MSM, various analytical methods including XRD, SEM, FTIR and *in vitro* cytotoxicity experiments were employed to assess the safety of the micro particles.

MATERIALS AND METHODS

Materials

Tetraethyl orthosilicate (TEOS), sodium hydroxide (NaOH), dichloromethane (HPLC grade) and cetyltrimethyl ammonium bromide (CTAB) were obtained from the Dae-Jung Chemicals (City: Korea) and utilized exactly as they were delivered. In-house deionized water was produced throughout the duration of the tests.

Preparation of MSNs

In order to create the mesoporous silica micro particles, the previously described procedure was modified (Mehmood *et al*., 2022c, Nunes *et al*., 2002). In essence, distinct sol-gels were created by methodically adjusting the water to dichloromethane ratio (1:1, 1:2, 2:1, 1:0 and 0:1) in the first phase of experiments. Each mixture (100mL) was added to a 250 mL volumetric flask, which had a constant temperature of 25°C. The pH was raised to 10.0 by adding 1mL of 0.5 M sodium hydroxide to the solution. Once a clear solution was produced, 500mg of CTAB was gradually added to the mixture and stirred on a magnetic stirrer at a speed of 1000 rpm. After thorough surfactant mixing, 10mL of TEOS was gradually added using a 10mL syringe and the mixture was continuously stirred for an hour at 25°C. The fluid became opaque after about 15minutes, suggesting that the reaction had begun and that white gel was starting to form. The white gel was washed three times with deionized water, filtered using a Sartorius filter of 0.2, and then allowed to dry for 8 hours at room temperature in a desiccator. To entirely eliminate the surfactant template, the dried bulk was then calcined at 500°C for 6 hours (Yoon *et al*., 2007). In this investigation, the formulations were referred to as MSM-1 through MSM-5.

Characterization of MSM

Morphology of MSM

The surface, shape and estimated size of MSM (VEGA3, TESCAN) were examined using scanning electron microscopy (SEM). Double adhesive tape was used to carefully attach mesoporous particles to a specimen holder. Various resolutions of micrographs were taken after the samples were dried and coated with gold.

Wide-angle X-ray diffraction

To generate the X-ray diffraction patterns for the specific sample, a combination of a CuK radiation source running at 30mA and 30 kV was employed in conjunction with an X-ray diffracto meter (Malvern Panalytical-X'pert PRO, UK). The data acquisition involved a step size of 0.02° and a scanning speed of 4°/min, covering a 2θ angle range from 10° to 40°.

FTIR spectroscopy

FTIR spectroscopy was utilized to examine potential interactions among the various components employed in synthesizing the mesoporous particles. Furthermore, it aimed to identify the silicate group present in the most optimal particles. Thermo Scientific, USA's Nicolet IS7ATR-FTIR spectrometer was utilized to acquire FTIR spectra with a resolution of $2cm^{-1}$ covering the 500 to $4000cm^{-1}$ spectral area.

In vitro cell viability studies

HepG2 cell line (ATCC; Manassas; produced at the University of Lahore) is now available thanks to the American Type Culture Collection. Cells were kept alive in DMEM enriched with 10% (v/v) FBS, humidity 95% (v/v), and 5% (v/v) CO_2 at 37°C. The MTT (3-(4,5-dimethylthiazol-2-yl)-2,5-diphenyltetrazolium bromide) test, which measures cell survival and proliferation, was used to determine the succinate dehydrogenase mitochondrial activity. (Mehmood *et al*., 2022c). The cell media received additions of MSM-1 through MSM-5 for 24 hours at the same rates (500mg/mL). Then, each well received 15µl of MTT (5mg/mL) in phosphate-buffered saline (PBS), and the wells underwent a further 4 hours of incubation at 37°C. Produced formazan crystals in each well were dissolved in 100µl of dimethyl sulfoxide (DMSO) after the solution containing MTT had been thoroughly aspirated. The absorbance at 570 nm of the dissolved formazan crystals was then determined using a micro plate reader. (Patel *et al*., 2009). The following formula was used to get the cell viability percentage.

$$\%\ \text{cell viability} = \frac{\text{Abs of treated cell} - \text{Abs of Blank}}{\text{Absof Control} - \text{Abs of Blank}} \times 100$$

STATISTICAL ANALYSIS

The statistical analysis was performed using the Graph-Pad Prism V.5 program. The data (SD) were represented using the mean and standard deviation. The threshold for statistical significance was a P value of 0.05 and 0.001.

RESULTS

Morphology of MSM

The majority of the formulations produced spherical MSM, according to SEM pictures, however, the size and

shape varied depending on the dichloromethane-water ratio. However, when we decreased the water content in the reaction mixture, MSM were large in size and were in a spherical shape. Even in fig. E we did not see any particles because only dichloromethane was used. When the ratio of dichloromethane to water in the MSM-3 formulations was equal, we produced the tiniest particles with a spherical shape (2:1) (fig. C). However, when we gradually changed the dichloromethane contents, no obvious trend in particle size was seen. Even when we used only water in reaction, there were no spherical particles produced. It is remarkable that when dichloromethane was the only reaction medium, no MSM were produced. MSM-3 was chosen as the optimal formulation.

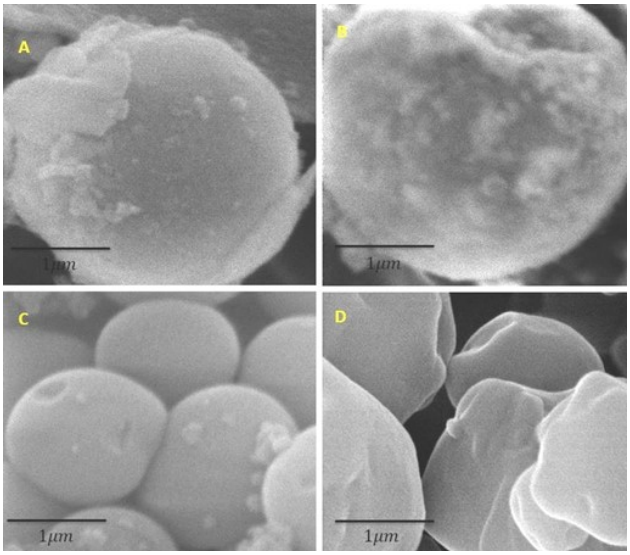

Fig. 1: SEM images of various mesoporous silica micro particles MSM-1(A), MSM-2(B), MSM-3 (C) and MSM-4 (D)

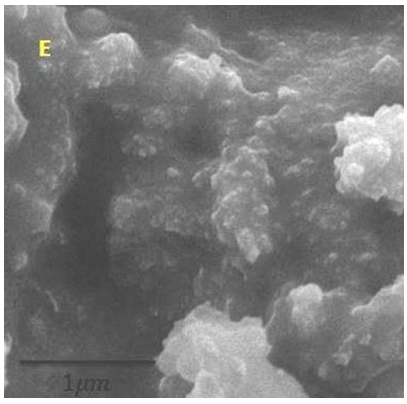

Fig. 2: SEM images of mesoporous silica micro particles MSM-5 (E).

FTIR spectroscopy

FTIR spectroscopy was utilized to examine the generated MSM for the purpose of confirming its identity and characterizing the functional groups found on silica particles, as depicted in fig. 3. The distinctive absorption bands of the MSM, observed at 797, 1053, 1636 and 3396 cm^{-1}, are occasionally associated with specific features such as the presence of siloxane linkages (797.97) (Wardhani *et al*., 2017), Si-O-Si bending (1053.78 cm^{-1}), silanol (Si-OH) symmetric stretching (3396.49) (Liu *et al*., 2015, Sevimli and Yılmaz, 2012) and bending vibrations at 1636 cm^{-1} (Liu *et al*., 2015, Wardhani *et al*., 2017). Broad bands at 3430cm^{-1} and 3454cm^{-1} are linked to O-H stretching, and bands at approximately 1625cm^{-1} can be linked to water O-H bending in the case of all formulated silica frameworks. All micro particles MSM-1 to MSM-5 showed the same peaks with different intensities. Thus, the FTIR spectra testified to the purity of the synthesized samples.

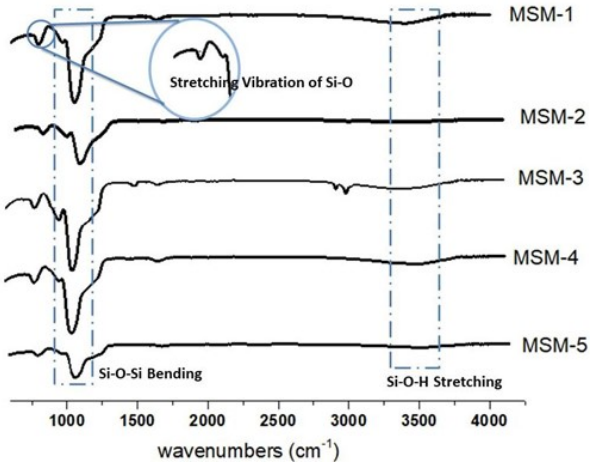

Fig. 3: FTIR spectrum of mesoporous silica Micro particles.

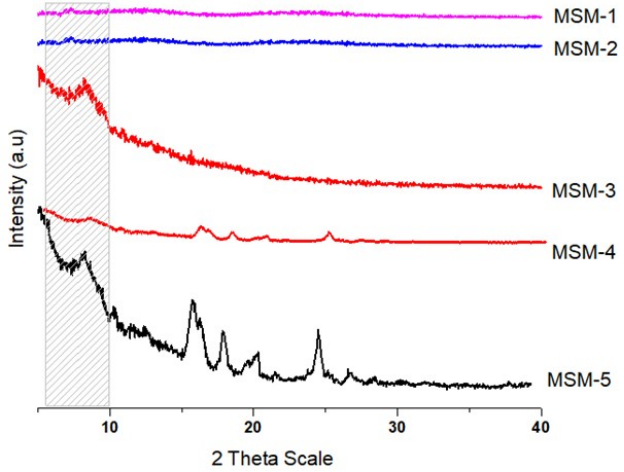

Fig. 4: XRD pattern of selected mesoporous silica Micro particles (MSM).

Wide-angle X-ray diffraction

Wide-angle X-ray diffraction was utilized to examine the crystalline and amorphous properties of the MSM-1 to MSM-5. Three diffraction peaks are produced by the MSM in the XRD study, which is used to identify the

particles as mesoporous silica (Lai *et al*., 2003, Slowing *et al*., 2006). The produced SiO2 samples' amorphous nature was confirmed by the X-ray diffraction patterns, as shown in fig. 4. The amorphous nature of MSM-1, MSM-2, and MSM-3 was confirmed by two large peaks seen at 25° and 10°. (Ghani, Saeed *et al*., 2017, Huo, Ouyang *et al*., 2014), as depicted in fig. 4. Different diffraction peaks were observed in MSM-4 and NAM-5. MSM-4 displayed two diffraction peaks, which indicated its non-order structure. Diffraction peaks at (100, 110 and 200) emerged at 2θ. These peaks were in accordance with the literature. Same peaks with high diffractions were seen in MSM-5 along with other multiple peaks. Once the peaks positioned shifted from the standard place, it indicated the degree of order reduced.

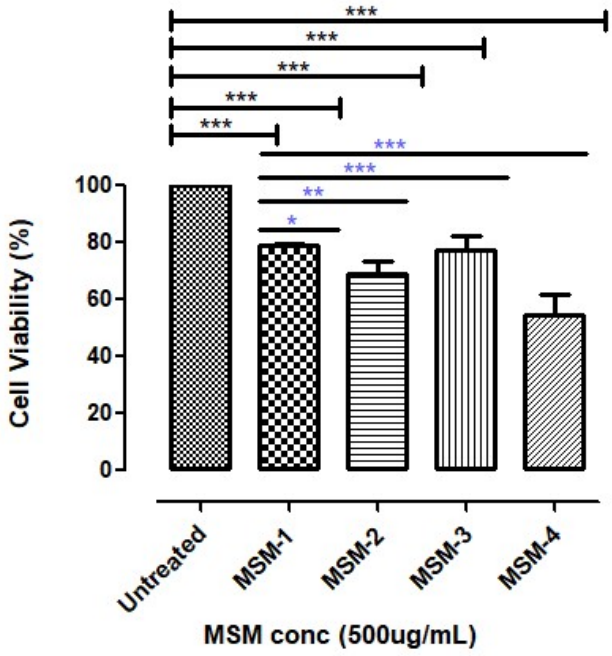

Fig. 5: Cell viability after exposure of silica micro particles for 24 hours. Black asterisk show comparison between untreated and treated cells. Blue asterisk shown comparison between MSM-1 to MSM-4 Where * = p<0.05, ** = p<0.005 and *** = p<0.001. When compared with untreated significant reduction in cell viability was observed in MSN-3.

In vitro toxicity testing

Using a human-derived hepatoma cell line (HepG2), *in vitro* cell viability (MTT assay) investigations employing four different formulations MSM-1 to MSM-4 (500µg/mL) were carried out. HepG2 cells treated with the formulation and exposed to a high concentration (500µg/mL) of all MSM particles, which had reduced cell viability (fig. 5). The production of MSM-3 using a ratio of water and dichloromethane (2:1) appears to be nearly harmless and biocompatible. The percent toxicity generated by MSM at concentrations (500µg/mL) was correspondingly 20.47 1.13, 27.11 5.56, 30.00 7.48, 39.63 8.17 and 53.31 1.86g/mL, suggesting a dose-dependent cytotoxic pattern. MSM-3 50% inhibitory concentration (IC_{50}) against HepG2 cells after 24 hours of exposure was calculated to be 776.2µg/mL, demonstrating the substance's comparatively low toxicity.

DISCUSSION

In order to produce MSM of controllable size and shape, we present a simple one-step synthesis approach for MSM that involves reacting TEOS with positively charged CTAB and dichloromethane-water combination at varied proportions under standard circumstances. To examine the impact of the solvent/co-solvent concentration on the prepared MSM, the ratio of dichloromethane to water was systematically changed. In order to create dichloromethane-water combinations with the requisite qualities, five experiments were carried out in one set. We gradually increased the amount of water in the dichloromethane. The amount of CTAB in the experimental sets was fixed at 500mg. As previously documented, the micellization process of different surfactants can be impacted by the presence of additives such co-solvents, which can also enhance or decrease the CMC (Dey *et al*., 2017, Rajput *et al*., 2016). According to Jalali and Gerandaneh (2011), different organic solvents have known impacts on CTAB CMC (Hoque *et al*., 2022); nonetheless, the amounts of CTAB used in our investigation were significantly greater than its CMC to create spherical micelles.

Once the critical micelle concentration is surpassed, the individual surfactant monomers undergo self-aggregation to form spherical micelles. By subjecting the negatively charged silica to the positively charged micelles under specific conditions, a range of MSMs with different sizes were effectively created. These conditions were determined based on the composition of the dichloromethane-water mixture. More intriguingly, the addition of TEOS made the reaction media opaque, allowing observers to see that the reaction speed increased as the amount of dichloromethane rose. The process proceeded with hydrolysis and subsequently TEOS condensation at the polar head region of CTAB micelles in the presence of NaOH, which served as a catalyst. The varied dichloromethane-water mixes determined the overall morphology of MSM, as demonstrated by the SEM figs. because to modest changes in micelle production in these mixtures, which eventually produced variances in the placement of the silica precursor at the top of the micellar template (fig. 1) (Vazquez *et al*., 2017).

The FTIR spectra provided confirmation of the presence of silicate in the produced MSM. Our findings are consistent with previous reports that demonstrate similar

FTIR results for MSM, further validating our results. (Maleki and Hamidi, 2016, Wardhani *et al*., 2017). The generation of MSM particles and their amorphous nature were additionally confirmed through XRD analysis, as these particles displayed two wide peaks at 10° and 25°, consistent with the description found in the existing literature.

CONCLUSIONS

In this study, using a straightforward sol-gel process and a variety of water and dichloromethane ratios, we effectively created MSM with a commendable yield. Proportions of water and dichloromethane (2:1) in the formulation produced homogenous, monodispersed particles with an average size of 1.0µm. These particles are compatible with cells in sufficient concentrations, according to *in vitro* cytotoxicity testing. In particular, its high yield, large surface area and tiny particle size, along with its comparatively quick synthesis, make it an appealing choice for pharmaceutical applications such as improving drug solubility, controlling drug release, and targeting.

REFERENCES

Anselmo AC and Mitragotri S (2019). Nanoparticles in the clinic: An update. *Bioeng. Transl. Med.*, **4**(3): e10143.

Brinker CJ and Scherer GW (2013). Sol-gel science: The physics and chemistry of sol-gel processing: Academic Press.

Dey A, Patra N, Mal A and Ghosh S (2017). Impact of organic polar solvents (DMSO and DMF) on the micellization and related behavior of an anionic (AOT), cationic (CEM2AB) and cationic gemini surfactant (16-5-16). *J. Mol. Liq.*, **244**: 85-96.

Ghani NNAMA, Saeed MA and Hashim IH (2017). Thermoluminescence (TL) response of silica nanoparticles subjected to 50 Gy gamma irradiation. *Mal. J. Fund. Appl. Sci.*, **13**(3): 178-180.

Graham T (1864). XXXV. On the properties of silicic acid and other analogous colloidal substances. *J. Chem. Soc.*, **17**: 318-327.

He Q, Zhang J, Shi J, Zhu Z, Zhang L, Bu W, Guo L and Chen Y (2010). The effect of PEGylation of mesoporous silica nanoparticles on nonspecific binding of serum proteins and cellular responses. *Biomaterials*, **31**(6): 1085-1092.

Hoque MA, Mahbub S, Khan MA and Eldesoky GE (2022). Interaction of sodium alginate with cetyltrimethylammonium bromide in aqua-organic mixed solvents: influence of temperatures and compositions. *J. Dispers. Sci.*, **43**(7): 1039-1047.

Huo C, Ouyang J and Yang H (2014). CuO nanoparticles encapsulated inside Al-MCM-41 mesoporous materials via direct synthetic route. *Sci. Rep.*, **4**(1): 3682.

Krajisnik D, Calija B and Cekic N (2017). Polymeric microparticles and inorganic micro/nanoparticulate drug carriers: An overview and pharmaceutical application. *Micro. Nano Carr. NSAIDs*, **2017**: 31-67.

Kumar P, Tambe P, Paknikar KM and Gajbhiye V (2018). Mesoporous silica nanoparticles as cutting-edge theranostics: Advancement from merely a carrier to tailor-made smart delivery platform. *JCR*, **287**: 35-57.

Lai C-Y, Trewyn BG, Jeftinija DM, Jeftinija K, Xu S, Jeftinija S and Lin VSY (2003). A mesoporous silica nanosphere-based carrier system with chemically removable CdS nanoparticle caps for stimuli-responsive controlled release of neurotransmitters and drug molecules. *J. Am. Chem. Soc.*, **125**(15): 4451-4459.

Li ZZ, Wen LX, Shao L and Chen JF (2004). Fabrication of porous hollow silica nanoparticles and their applications in drug release control. *J. Control Release*, **98**(2): 245-254.

Li Z, Zhang Y and Feng N (2019). Mesoporous silica nanoparticles: Synthesis, classification, drug loading, pharmacokinetics, biocompatibility and application in drug delivery. *Expert Opin. Drug Deliv.*, **16**(3): 219-237.

Liu F, Wang J, Huang P, Zhang Q, Deng J, Cao Q, Jia J, Cheng J, Fang Y and Deng DY (2015). Outside-in stepwise functionalization of mesoporous silica nanocarriers for matrix type sustained release of fluoroquinolone drugs. *J. Mater. Chem. B.*, **3**(10): 2206-2214.

Maggini L, Cabrera I, Ruiz-Carretero A, Prasetyanto EA, Robinet E and De Cola L (2016). Breakable mesoporous silica nanoparticles for targeted drug delivery. *Nanoscale*, **8**(13): 7240-7247.

Maleki A and Hamidi M (2016). Dissolution enhancement of a model poorly water-soluble drug, atorvastatin, with ordered mesoporous silica: comparison of MSF with SBA-15 as drug carriers. *Expert. Opin. Drug Deliv.*, **13**(2): 171-181.

Manzano M and Vallet-Regí M (2020). Mesoporous silica nanoparticles for drug delivery. *Adv. Funct. Mater.*, **30**(2): 1902634.

Mehmood Y, Khan IU, Shahzad Y, Khalid SH, Asghar S, Irfan M, Asif M, Khalid I, Yousaf AM and Hussain T (2019). Facile synthesis of mesoporous silica nanoparticles using modified sol-gel method: Optimization and *in vitro* cytotoxicity studies. *Pak. J. Pharm. Sci.*, **32**(4): 1805-1812.

Mehmood Y, Khan IU, Shahzad Y, Khan RU, Iqbal MS, Khan HA, Khalid I, Yousaf AM, Khalid SH. Asghar S (2020a). *In-vitro* and *in-vivo* evaluation of velpatasvir-loaded mesoporous silica scaffolds. A prospective carrier for drug bioavailability enhancement. *Pharmaceutics.*, **12**(4): 307.

Mehmood Y, Khan IU, Shahzad Y, Khan RU, Khalid SH, Yousaf AM, Hussain T, Asghar S, Khalid I and Asif M (2020b). Amino-decorated mesoporous silica nano-

particles for controlled sofosbuvir delivery. *Eur. J. Pharm. Sci.*, **143**: 105184.

Mehmood Y, Shahid H, Barkat K, Ibraheem M, Riaz H, Badshah SF, Chopra H, Sharma R, Nepovimova E and Kuca K (2022a). Designing of SiO2 mesoporous-nanoparticles loaded with mometasone furoate for potential nasal drug delivery: *Ex vivo* evaluation and determination of pro-inflammatory interferon and interleukins mRNA expression. *Front. Cell Dev. Biol.*, **10**(Jan 6): 2411.

Mehmood Y, Shahid H, Rashid MA, Alhamhoom Y and Kazi M (2022b). Developing of SiO2 nanoshells loaded with fluticasone propionate for potential nasal drug delivery: Determination of pro-inflammatory cytokines through mRNA expression. *J. Funct. Biomater.*, **13**(4): 229.

Mehmood Y, Shahid H, Tariq A and Ali SO (2022c). Efficacy and safety of a new mometasone furoate nasal spray formulation in patients with acute rhinosinusitis: A randomized clinical trial. *Ital. J. Med.*, **16**(1):10-14

Nunes CD, Valente AA, Pillinger M, Fernandes AC, Romao CC, Rocha J and Gonçalves IS (2002). MCM-41 functionalized with bipyridyl groups and its use as a support for oxomolybdenum (VI) catalysts. *J. Mater. Chem.*, **12**(6): 1735-1742.

Patel S, Gheewala N, Suthar A and Shah A (2009). In-vitro cytotoxicity activity of Solanum nigrum extract against Hela cell line and Vero cell line. *Int. J. Pharm. Pharm.*, **1**(1): 38-46.

Rajput SM, More UU, Vaid ZS, Prajapati KD and Malek NI (2016). Impact of organic solvents on the micellization and interfacial behavior of ionic liquid based surfactants. *Colloids Surf.*, **507**: 182-189.

Sevimli F. Yılmaz A (2012). Surface functionalization of SBA-15 particles for amoxicillin delivery. *Micropor. Mesopor. Mat.*, **158**: 281-291.

Singh LP, Bhattacharyya SK, Kumar R, Mishra G, Sharma U, Singh G and Ahalawat S (2014). Sol-Gel processing of silica nanoparticles and their applications. *Adv. Colloid. Interfac.*, **214**: 17-37.

Slowing I, Trewyn BG and Lin VSY (2006). Effect of surface functionalization of MCM-41-type mesoporous silica nanoparticles on the endocytosis by human cancer cells. *J. Am. Chem. Soc.*, **128**(46): 14792-14793.

Sur S, Rathore A, Dave V, Reddy KR, Chouhan RS and Sadhu V (2019). Recent developments in functionalized polymer nanoparticles for efficient drug delivery system. *Nano-Struct.*, **20**: 100397.

Tang F, Li L and Chen D (2012). Mesoporous silica nanoparticles: Synthesis, biocompatibility and drug delivery. *Adv. Mater.*, **24**(12): 1504-1534.

Vazquez NI, Gonzalez Z, Ferrari B and Castro Y (2017). Synthesis of mesoporous silica nanoparticles by sol-gel as nanocontainer for future drug delivery applications. *Bol. Soc. Esp. Ceram. V.*, **56**(3): 139-145.

Vivero-Escoto JL, Slowing II and Lin VSY (2010). Tuning the cellular uptake and cytotoxicity properties of oligonucleotide intercalator-functionalized mesoporous silica nanoparticles with human cervical cancer cells HeLa. *Biomaterials*, **31**(6): 1325-1333.

Wardhani GAPK, Nurlela N and Azizah M (2017). Silica content and structure from corncob ash with various acid treatment (HCl, HBr and Citric Acid). *Molekul*, **12**(2): 174-181.

Xu C, Yu M, Noonan O, Zhang J, Song H, Zhang H, Lei C, Niu Y, Huang X and Yang Y (2015). Core-cone structured monodispersed mesoporous silica nanoparticles with ultra-large cavity for protein delivery. *Small.*, **11**(44): 5949-5955.

Yoon SB, Kim JY, Kim JH, Park YJ, Yoon KR, Park SK and Yu JS (2007). Synthesis of monodisperse spherical silica particles with solid core and mesoporous shell: Mesopore channels perpendicular to the surface. *J. Mater. Chem.*, **17**(18): 1758-1761.

Zhang Y, Yue Q, Zagho MM, Zhang J, Elzatahry AA, Jiang Y and Deng Y (2019). Core-shell magnetic mesoporous silica microspheres with large mesopores for enzyme immobilization in biocatalysis. *ACS Appl. Mater. Interfaces.*, **11**(10): 10356-10363.

Zhou Y, Quan G, Wu Q, Zhang X, Niu B, Wu B, Huang Y, Pan X and Wu C (2018). Mesoporous silica nanoparticles for drug and gene delivery. *Acta Pharmaceutica Sinica B.*, **8**(2): 165-177.